



Cite this: *Green Chem.*, 2022, **24**, 8447

## Optimisation of PET glycolysis by applying recyclable heterogeneous organocatalysts†

Zsuzsanna Fehér,<sup>a</sup> Johanna Kiss,<sup>a</sup> Péter Kisszékelyi,<sup>a</sup> János Molnár,<sup>b</sup> Péter Huszthy,<sup>a</sup> Levente Kárpáti<sup>b</sup> and József Kupai<sup>\*,a</sup>

Chemical depolymerisation, or solvolysis, can be a sustainable plastic recycling method, as a circular economy can be achieved by recovering the pure monomers. Polyethylene terephthalate (PET) is a ubiquitous plastic material with short-life application and slow biodegradation, so its waste management needs to be continuously improved. In this study, we tested three commercially available organocatalyst-modified silica gels in the glycolysis of PET and developed another, functionalized with triazabicyclodecene (TBD), which was also tested. Organocatalysts are efficient in PET glycolysis, but their recyclability needs to be improved for industrial application. The applied heterogeneous modified silica gels can be recovered easily by filtration. Si-TEA catalyst was chosen for reaction optimisation because it has the highest thermal stability and good catalytic activity. The PET glycolysis process was optimised by fractional factorial experimental design and response surface methodology. Under optimal reaction conditions (PET (384 mg, 2 mmol), ethylene glycol (1.41 mL, 25.2 mmol), Si-TEA (15.5 mol%), 190 °C, 1.7 h), 88.5% non-isolated bis(2-hydroxyethyl) terephthalate (BHET) monomer yield was obtained. Si-TEA and Si-TBD catalysts were recycled in five reaction cycles, and with both catalysts, high cumulative BHET yields (89 and 88%, respectively) were achieved. Additionally, environmental energy impacts were calculated for the two catalysts and were compared favourably with other organocatalysts in the literature. A process scale-up was also implemented. Finally, it has been verified that modified silica gels have much higher catalytic activities than native silica gel, as solvolytic reactions using the former catalysts took a significantly shorter time.

Received 1st August 2022,  
Accepted 11th October 2022

DOI: 10.1039/d2gc02860c

rsc.li/greenchem

## 1 Introduction

As global plastic production increases exponentially,<sup>1</sup> there is a growing demand for environmental awareness and sustainable plastic recycling methods. Amongst the most prevalent plastic materials, polyethylene terephthalate (PET) is the one that becomes waste in the highest proportion of its produced quantity (97% of 33 million tons in 2015<sup>1</sup>). This is because PET is primarily used as a short-life packaging material.<sup>2</sup> Because of its slow biodegradation and inadequate waste management, adaptive and well-designed recycling strategies are needed to prevent plastic's harmful effect on the environment and improve the sustainability of plastic use.<sup>3</sup>

Plastic recycling methods fall into four categories: primary (industrial scrap recycling), secondary (mechanical), tertiary (chemical), and quaternary (incineration) recycling.<sup>4</sup> Mechanical recycling is still considered the most favourable due to its lower energy requirement than chemical recycling. In the case of PET bottles, the mechanical recycling technology is indispensable, particularly when there is a deposit refund system that can provide clean, homogeneous material for bottle-to-bottle recycling.<sup>5</sup> However, if there is no such possibility, chemical recycling can be adapted in the case of contaminated, heterogeneous waste streams. Chemical recycling can be split into three categories: solvent purification, chemical depolymerisation (solvolysis or chemolysis), and thermal depolymerisation (thermal cracking or thermolysis). Among these technologies, solvolysis, which means the depolymerisation of plastic waste into its monomers and oligomers by a nucleophile reagent acting also as the solvent,<sup>6</sup> has the most promise to complement mechanical recycling. This is because it can live up to the demands made for chemical recycling that mechanical recycling sometimes struggles to achieve: infinite virgin-grade recycling is technically feasible, food-grade products can be produced, and the removal of contaminants is

<sup>a</sup>Department of Organic Chemistry and Technology, Faculty of Chemical Technology and Biotechnology, Budapest University of Technology and Economics, Műegyetem rkp. 3., H-1111 Budapest, Hungary. E-mail: kupai.jozsef@vbk.bme.hu

<sup>b</sup>Laboratory of Plastics and Rubber Technology, Faculty of Chemical Technology and Biotechnology, Budapest University of Technology and Economics, Műegyetem rkp. 3., H-1111 Budapest, Hungary

† Electronic supplementary information (ESI) available. See DOI: <https://doi.org/10.1039/d2gc02860c>





ground into small flakes (thickness  $0.41 \pm 0.08$  mm;  $(9.9 \pm 2.9$  mm)  $\times$   $(6.8 \pm 2.2$  mm)). Modified silica gels (Si-TEA, Si-GUA, Si-THU, silica gel functionalized with glycidoxo groups (Si-GLY)) were purchased from SiliCycle Inc, the unmodified silica gel (Si) and toluene from Merck. Ethylene glycol and TBD were purchased from Sigma-Aldrich.

## 2.2 Preparation of TBD-modified silica gel (Si-TBD)

Si-GLY (5 g, 5.55 mmol glycidyl group), toluene (45 mL), and TBD (927 mg, 6.66 mmol) were added to a two-necked round-bottomed flask. The reaction mixture was stirred under argon atmosphere and heated under reflux for 10 hours. The solid product was filtered on a sintered glass filter and washed with a mixture of dichloromethane/methanol 5 : 1 (15 mL), followed by a mixture of dichloromethane/methanol/triethylamine 5 : 1 : 0.05 ( $2 \times 15$  mL), then again with dichloromethane/methanol 5 : 1 ( $2 \times 15$  mL). The product was dried in a drying oven at 80 °C for 2 hours to give a mass of 5.36 g—the molecular loading of Si-TBD was  $0.58 \pm 0.09$  mmol  $g^{-1}$ , determined by SEM-EDX elemental analysis.

## 2.3 General procedure for PET glycolysis

The catalyst, PET flakes (384 mg, 2 mmol), and ethylene glycol were added to a 5 mL sealable vial. The reagent and catalyst ratios were calculated in relation to the amount of PET repeating unit (MW = 192.2  $g\ mol^{-1}$ ). The reactions were carried out under argon atmosphere, and magnetic stirring was used. A sand bath was used for heating, and the internal temperature (170–195 °C) was monitored by a thermometer placed in a separate 5 mL sealed vial filled with ethylene glycol. After the appropriate reaction time (1–2 h), the reaction mixture was allowed to cool to room temperature, and then HPLC samples were prepared to determine the non-isolated BHET yield. A MeCN : H<sub>2</sub>O = 5 : 1 mixture ( $3 \times 2$  mL) was added to the reaction mixture and filtered on a sintered glass filter to separate the catalyst and any remaining solid oligomers from the desired product. The solid residue was washed with MeCN : H<sub>2</sub>O = 5 : 1 solvent mixture ( $3 \times 3$  mL). The filtrate was then transferred to a 25 mL volumetric flask and filled with the above-mentioned solvent mixture to 25 mL. For the HPLC sample, 50  $\mu$ L of this solution was taken, and 950  $\mu$ L of MeCN : H<sub>2</sub>O = 5 : 1 solvent mixture was added.

The BHET was isolated by analogy with the method of Zhang and co-workers.<sup>44</sup> For determining the isolated BHET yield, the acetonitrile was removed from the filtrate (MeCN : H<sub>2</sub>O = 5 : 1 mixture containing BHET, EG, and BHET dimer/trimer by-products) under reduced pressure, and the volume of the remaining aqueous solution was extended by water to 70 mL. Then, the water-insoluble oligomers (dimer and, in some cases, trimer based on HPLC-MS) were removed by filtration using a filter paper, and the filtrate was evaporated to approx. 4 mL under reduced pressure. The resulting solution was stored for 12 hours in a refrigerator (4 °C) to give BHET as white crystals. These crystals were filtered on a sintered glass filter and washed with the mother liquor, then with water.

The main product was identified by <sup>1</sup>H, <sup>13</sup>C nuclear magnetic resonance spectroscopy (NMR), high-resolution mass spectrometry (HRMS), and Fourier-transform infrared spectroscopy (FTIR), and the BHET dimer side-product was identified by <sup>1</sup>H, <sup>13</sup>C NMR, and HRMS.

**BHET.** Melting point: 109 °C. Spectroscopic data (see Fig. S1–S4 in the ESI†) are fully consistent with those reported in the literature.<sup>23</sup> <sup>1</sup>H NMR (500 MHz, DMSO-*d*<sub>6</sub>):  $\delta$  8.12 (s, 4H, CH), 4.98 (t,  $J = 5.7$  Hz, 2H, OH), 4.32 (t,  $J = 4.9$  Hz, 4H, O-CH<sub>2</sub>), 3.72 (q,  $J = 5.1$  Hz, 4H, CH<sub>2</sub>-OH) ppm. <sup>13</sup>C NMR (126 MHz, DMSO-*d*<sub>6</sub>):  $\delta$  165.2, 133.8, 129.6, 67.1, 59.0 ppm. IR (KBr):  $\nu_{\max}$  3447, 2964, 2946, 2932, 2880, 1716, 1689, 1505, 1457, 1412, 1380, 1282, 1252, 1135, 1111, 1074, 1017, 910, 898, 875  $cm^{-1}$ . HRMS (ESI<sup>+</sup>):  $m/z$  [M + Na]<sup>+</sup> calcd for C<sub>12</sub>H<sub>14</sub>O<sub>6</sub>Na: 277.0688; found: 277.0689.

**BHET dimer.** Melting point: 162–166 °C. To the best of our knowledge, the spectroscopic data of the dimer has not been reported so far (see Fig. S5–S6 in the ESI†). <sup>1</sup>H NMR (500 MHz, DMSO-*d*<sub>6</sub>):  $\delta$  8.12 (dd,  $J = 13.5$  Hz, and 8.5 Hz, 8H, CH), 4.95 (t,  $J = 5.7$  Hz, 2H, OH), 4.68 (s, 4H, O-CH<sub>2</sub>-CH<sub>2</sub>-O (middle)), 4.31 (t,  $J = 5.0$  Hz, 4H, O-CH<sub>2</sub> (next to CH<sub>2</sub>-OH)), 3.71 (q,  $J = 5.1$  Hz, 4H, CH<sub>2</sub>-OH) ppm. <sup>13</sup>C NMR (126 MHz, DMSO-*d*<sub>6</sub>):  $\delta$  165.1, 165.0, 133.9, 133.3, 129.6, 129.5, 67.0, 63.2, 59.0 ppm. HRMS (ESI<sup>+</sup>):  $m/z$  [M + Na]<sup>+</sup> calcd for C<sub>22</sub>H<sub>22</sub>NaO<sub>10</sub>: 469.1105; found: 469.1102.

BHET yield (non-isolated) was calculated based on HPLC calibration method using an external standard, by fitting a line to five data points (see Fig. S11 in the ESI†). The non-isolated yield was also compared with the isolated yield in some cases. The isolated yield was calculated as

$$\text{Yield}[\%] = \frac{m_{\text{BHET}}}{m_{\text{BHET},0}} \times 100\% \quad (1)$$

where  $m_{\text{BHET}}$  and  $m_{\text{BHET},0}$  refer to the actual and theoretical mass of BHET, respectively. The theoretical weight of BHET was calculated by

$$m_{\text{BHET},0} = \frac{m_{\text{PET},0}}{192.2} \times 254.2 \quad (2)$$

where  $m_{\text{PET},0}$  is the initial mass of PET; 192.2 and 254.2 are the molecular weight of the PET repeating unit and BHET, respectively.

PET conversion was calculated as

$$\text{Conversion}[\%] = \left( 1 - \frac{m_r - m_{c,0}}{m_{\text{PET},0}} \right) \times 100\% \quad (3)$$

where  $m_r$  and  $m_{c,0}$  refer to the mass of the solid residue and the initial mass of the catalyst, respectively.

## 2.4 Catalyst recycling

For the catalyst recycling, 5 reaction cycles were carried out with Si-TEA and Si-TBD catalysts under optimal conditions. Each cycle was repeated once. To maintain the optimal ratio of the parameters, the mass of PET and the amount of ethylene glycol were reduced in proportion to the mass of the recycled catalyst. If the reaction did not proceed with complete conver-



sion, the solid residue remaining after filtration was transferred to the next reaction cycle.

## 2.5 Scale-up of PET glycolysis process

**6-fold scale-up.** The catalyst (15.5 mol% Si-TEA or 50 wt% Si), PET flakes (2.31 g, 12 mmol), and ethylene glycol (12.6 eq.) were added to a 50 mL round-bottomed flask. The reactions were carried out under argon atmosphere, and magnetic stirring was used. An oil bath was used for heating. When the reaction was completed, the reaction mixture was allowed to cool to room temperature. A MeCN:H<sub>2</sub>O = 5:1 mixture (15 mL) was added to the reaction mixture and filtered on a sintered glass filter to separate the catalyst and any remaining solid oligomers from the desired product. The solid residue was washed with the above-mentioned solvent mixture (3 × 5 mL). The acetonitrile was removed from the filtrate under reduced pressure, and the volume of the remaining aqueous solution was extended by water to approx. 420 mL. The water-insoluble oligomers (dimer and trimer) were removed by filtration using a filter paper, and the filtrate was evaporated to approx. 25 mL under reduced pressure. The resulting solution was stored for 12 hours in a refrigerator (4 °C) to give BHET as white crystals. These were filtered on a sintered glass filter and washed with the mother liquor, then with water.

**18-fold scale-up.** The catalyst (15.5 mol% Si-TEA), PET flakes (7.00 g, 36.4 mmol), and ethylene glycol (12.6 eq.) were added to a 100 mL flat-bottomed flask. The reaction was carried out under argon atmosphere, and mechanical stirring (800 rpm) was used. An oil bath was used for heating. The reaction was completed after 5 hours, and the reaction mixture was allowed to cool to room temperature, and then an HPLC sample was prepared to determine the non-isolated BHET yield. A MeCN:H<sub>2</sub>O = 5:1 mixture (20 mL) was added to the reaction mixture and filtered on a sintered glass filter to separate the catalyst and any remaining solid oligomers from the desired product. The solid residue was washed with the above-mentioned solvent mixture (6 × 20 mL). The filtrate was then transferred to a 500 mL volumetric flask and filled with the above-mentioned solvent mixture to 500 mL. For the HPLC sample, 60 μL of this solution was taken, and 940 μL of MeCN:H<sub>2</sub>O = 5:1 solvent mixture was added.

For determining the isolated BHET yield, the acetonitrile was removed from the filtrate (MeCN:H<sub>2</sub>O = 5:1 mixture containing BHET, EG, and by-products) under reduced pressure, and the volume of the remaining aqueous solution was extended by water to 1.3 L. Then, the water-insoluble oligomers (dimer and trimer) and smaller-sized catalyst fraction (see Section 3.5) were removed by filtration using a filter paper (the solid residue on the filter paper was washed with a methanol:ethyl acetate = 1:1 mixture to recover the smaller-sized catalyst fraction by dissolving the oligomers), and the filtrate was evaporated to approx. 53 mL under reduced pressure. The resulting solution was stored for 12 hours in a refrigerator (4 °C) to give BHET as white crystals. These crystals were filtered on a sintered glass filter and washed with the mother liquor, then with water.

HPLC was performed using a Shimadzu LCMS-2020 device equipped with a HALO C18 (2.7 μm; 4.6 × 150 mm) column. The samples were eluted with gradient elution, using eluent A (0.1% HCOOH in H<sub>2</sub>O) and eluent B (MeCN). The flow rate was set to 0.8 mL min<sup>-1</sup>. The initial condition was 5% eluent B, followed by a linear gradient to 100% eluent B by 8 min; from 8 to 13 min, 100% eluent B was retained; and from 13 to 14 min, it went back by a linear gradient to 5% eluent B, which was retained from 14 to 15 min. The column temperature was kept at 40 °C, and the injection volume was 1 μL.

## 2.6 Experimental design

The optimisation of PET glycolysis was conducted by response surface methodology with gradient method. Statistica software (TIBCO Software Inc.) was applied for data analysis at 5% significance level (to calculate the regression model and perform analysis of variance (ANOVA)). 2<sup>4-1</sup> fractional factorial design was applied with two centre point experiments, and all experiments were repeated once. The effects of four independent variables (*i.e.*, reaction temperature, catalyst:PET ratio in mol%, EG:PET molar ratio, and reaction time) were investigated. Two dependent variables were chosen as responses, BHET yield (*Y*) and PET conversion.

## 2.7 Characterisation

Infrared spectra were recorded on a Bruker Alpha-T FTIR spectrometer. Silica gel 60 F<sub>254</sub> (Merck) plates were used for thin-layer chromatography (TLC). Ratios of solvents are given in volumes (mL mL<sup>-1</sup>). Melting points were measured in a Boetius micro-melting point apparatus, and were uncorrected.

NMR spectra were recorded on a Bruker Avance 500 MHz spectrometer (500.13 MHz for <sup>1</sup>H, 125.76 MHz for <sup>13</sup>C) in DMSO-d<sub>6</sub> and were referenced to residual solvent proton signals (δ<sub>H</sub> = 2.50) and solvent carbon signals (δ<sub>C</sub> = 39.51). All chemical shifts are reported in parts per million (ppm). Coupling constants (*J*) are given in Hz.

HPLC-MS was performed using a Shimadzu LCMS-2020 device, equipped with a Reprospher 100 C18 (5 μm; 100 × 3 mm) column and a positive/negative double ion source (DUIS±) with a quadrupole MS analyser in a range of 50–1000 *m/z*. The samples were eluted with gradient elution, using eluent A (0.1% HCOOH in H<sub>2</sub>O) and eluent B (0.1% HCOOH in MeCN). The flow rate was set to 1.5 mL min<sup>-1</sup>. The initial condition was 5% eluent B, followed by a linear gradient to 100% eluent B by 1.5 min; from 1.5 to 4.0 min, 100% eluent B was retained; and from 4 to 4.5 min, it went back by a linear gradient to 5% eluent B, which was retained from 4.5 to 5 min. The column temperature was kept at 30 °C, and the injection volume was 1 μL. The purity of the compounds was assessed by HPLC with UV detection at 215 and 254 nm. High-resolution mass spectrometry was measured on a Q-TOF Premier mass spectrometer for BHET, and on a Bruker MicroTOF II instrument for the BHET dimer. The ionisation method was electrospray ionisation (ESI) operated in positive ion mode.

The stability of the catalysts was investigated by thermogravimetric analysis and differential scanning calorimetry



(TG-DSC). A PerkinElmer STA 6000 instrument was used. During the measurement, the samples of about 30 mg were heated from 25 °C to 190 °C at a heating rate of 10 °C min<sup>-1</sup> and then held at the latter temperature for 360 min.

Si-TBD was analysed using a JEOL JSM-5500LV scanning electron microscope (SEM) at high vacuum with 10–20 kV accelerating voltage. The elemental analysis of Si-TBD was carried out with energy dispersive X-ray analysis (EDX with Si (Li) detector) applying 10 kV accelerating voltage and sampling time of 40 s.

The physical properties of the commercially available functionalized silica gels (particle size – measured by laser diffraction, specific surface area – measured by nitrogen adsorption/desorption method at 77 K, molecular loading – measured by elemental analysis, or titration in the case of Si-GLY), which were given by the manufacturer, SiliCycle Inc, can be found in Table S1 in the ESI.†

HS-GC-MS was performed using a Shimadzu GCMS-QP2010 device equipped with an Rtx-5 (30 m × 0.32 mm × 0.25 μm) column and an AOC-5000 auto-injector. The oven temperature was initially held at 40 °C for 2 minutes, increased to 320 °C at 10 °C min<sup>-1</sup> with the final temperature held for 5 minutes. The sample holder was thermostated for 45 minutes at 190 °C before the measurement. The carrier gas was argon, the linear flow rate on the column was set to 50 cm s<sup>-1</sup>, and the split ratio was 1 : 10. The injector was held at 300 °C. The interface and the ion source temperature were set at 250 °C, the syringe temperature was 150 °C, and the detector voltage was 1.3 kV. Taking the molecular weights of the expected molecules into consideration, the mass scale was adjusted between mass to charge ratio (*m/z*) of 29–600.

## 3 Results and discussion

### 3.1 Synthesis and characterisation of catalysts

The Si-TBD was prepared from Si-GLY by reacting with TBD in toluene (Scheme 1). The Si-GLY used as starting material has a particle size of 40–63 μm, a specific surface area of 494 m<sup>2</sup> g<sup>-1</sup>, and an active loading (the molecular loading measured by titration by the manufacturer, SiliCycle Inc) of 1.11 mmol g<sup>-1</sup>. Then, leaching of TBD from the catalyst was investigated: the product was stirred in a solvent mixture (dichloromethane/methanol 5 : 1) in which TBD was highly soluble, filtered, and washed. Analysis of the filtrate by HPLC-MS showed that less than 5% of the TBD on the catalyst surface (based on molecular loading) leached off from the catalyst.

In addition to the synthesised Si-TBD, three commercially available functionalized silica gels, Si-GUA, Si-THU, or Si-TEA, were investigated (Fig. 1). The physical properties (particle size, specific surface area, molecular loading) of the commercially available functionalized silica gels, which were given by the manufacturer, SiliCycle Inc, can be found in Table S1 in the ESI.† To find the catalyst with the highest catalytic activity and recyclability while preserving the catalytic activity among the modified silica gels tested, we investigated their thermal stability by thermogravimetric analysis and differential scanning calorimetry (TG-DSC), being held at 190 °C (the temperature which is most commonly used in PET glycolysis) for 360 min. From the TG curves, which are similar for each tested silica gel (see Fig. S7–S10 in the ESI†), the mass loss of each sample was determined. For each of the modified silica gels, a theoretical mass loss was also calculated based on the molecular loading, assuming that all the organic units are eliminated from the modified silica gel. The theoretical and measured mass losses of the catalysts are summarised in Table 1. Since Si-TEA showed the lowest mass loss in the TG-DSC measurement, it is assumed to have the highest thermal stability. Si-TBD also showed a much lower mass loss than the theoretical maximum.

During our experiments, the reactions are conducted in inert atmosphere. Otherwise, the tertiary amines in the catalysts could react with oxygen to give *N*-oxides, and then the Cope elimination of *N*-oxides would produce alkenes. There was no significant degradation of the catalysts observed. The thermal stability of silica gel-supported organocatalysts was reported earlier.<sup>45</sup>

The morphology of the Si-TBD catalyst was investigated by SEM. Comparing its SEM image (Fig. 2(a)) with the starting

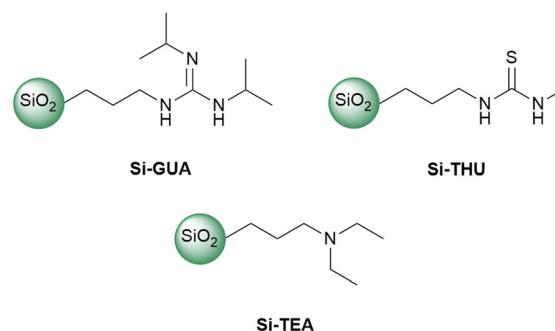


Fig. 1 The applied, commercially available functionalized silica gels.

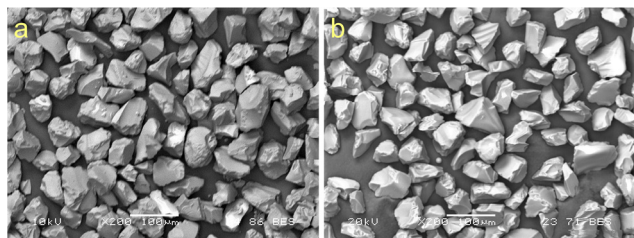


Scheme 1 Preparation of TBD-functionalized silica gel.



**Table 1** Theoretical and measured mass losses of the catalysts measured by TG-DSC (190 °C, 6 h)

Modified silica gels	Mass loss (%)		Measured/theoretical maximum ratio (%)
	Theoretical maximum	Measured	
Si-GUA	16	12	75
Si-TEA	10	2	25
Si-THU	11	8	73
Si-TBD	15	8	53

**Fig. 2** SEM images of Si-TBD (a) and Si-GLY (b).

material, Si-GLY (Fig. 2(b)), both modified silica gels have irregular particle shapes with similar particle sizes. Therefore, it can be assumed that the particle size distribution did not change during the modification of Si-GLY (40–63 μm, measured by laser diffraction by SiliCycle Inc for Si-GLY). The molecular loading of Si-TBD was determined by SEM-EDX analysis based on nitrogen content. Si-GLY was used as background for the calculation.

### 3.2 Catalyst screening

TBD is a bifunctional catalyst that can activate both an ester and alcohol through hydrogen bonding.<sup>46</sup> Numerous nitrogen-based organocatalysts were screened for the depolymerisation of PET earlier in the literature.<sup>25,47</sup> The catalytic activity was found to correlate with the basicity, but in the presence of short-chain diols such as ethylene glycol, which serve as a cocatalyst for activating the ester carbonyl groups *via* hydrogen bonding, the bifunctionality of TBD is less important, especially in the presence of excess ethylene glycol.<sup>25</sup> The synthesised catalyst, Si-TBD loses the bifunctionality because of the grafting onto silica support (and thus, its basicity decreases – based on the reported  $pK_a$  of the conjugated acid of methyl-TBD<sup>48</sup>), but as we use excess ethylene glycol, this

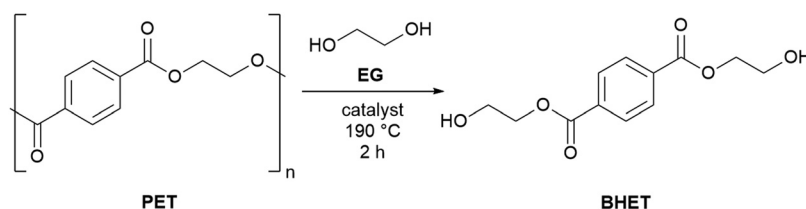
probably does not hinder the catalytic activity greatly because of the latter findings. Thus, we wanted to screen other silica gel-grafted nitrogen-based organocatalysts also, that can be easily accessed commercially, so we chose based on literature analogies: Si-TEA based on triethylamine,<sup>49</sup> Si-THU based on urea<sup>44</sup> and another guanidine-based catalyst presumably similar to Si-TBD, Si-GUA.

The catalytic activities of the commercially available modified silica gels (Si-GUA, Si-TEA, Si-THU, with a particle size of 40–63 μm) and the newly synthesised Si-TBD were investigated in PET glycolysis (Scheme 2), and the results are shown in Fig. 3. In addition to the modified silica gels, unmodified silica gel (Si, also with a particle size of 40–63 μm) was also tested, and reactions without catalyst were also performed. The depolymerisation rate was low without catalyst (9% conversion), while it was slightly higher (34% conversion, 26% BHET yield) with Si. Thus, even the silica support has catalytic activity, but much lower than those of the modified silica gels: the three modified silica gels containing basic units (Si-TBD, Si-GUA, Si-TEA) showed excellent catalytic activities and selectivities (96–100% PET conversions, 83–92% BHET yields) with relatively low standard deviation. Applying the Si-THU catalyst, high deviation was observed supposedly because of the catalyst's instability at high temperature. As the aim was to recycle the catalyst in as many cycles as possible, Si-TEA was chosen as the best catalyst for further reactions because of its relatively high catalytic activity and good thermal stability based on the TG-DSC measurements (see Table 1).

To confirm the advantages of the Si-TEA modified silica gel catalyst, triethylamine (TEA) was also applied as a catalyst. TEA should only be used in a closed reaction vessel; otherwise, it will evaporate from the reaction mixture. The latter catalyst also gave an excellent non-isolated yield (91%), but the remaining triethylamine traces in the reaction mixture probably hindered the crystallization of BHET, as a poorer isolated yield (69%) was obtained than with the heterogeneous catalysts. To demonstrate the difference, in one case when Si-TEA was used, a non-isolated yield of 90% was observed with an isolated yield of 85%.

### 3.3 Regression model based on experimental design

The effects of four independent variables (*i.e.*, reaction temperature, catalyst : PET ratio in mol%, EG : PET molar ratio, and reaction time) were investigated as quantitative factors most frequently studied in the literature on glycolysis of PET. The aim was to set up a simple model with relatively few experi-

**Scheme 2** PET glycolysis with EG using different catalysts.



**Fig. 3** The catalytic activities of different catalysts in PET glycolysis. Reaction conditions: 190 °C, 10 mol% (or 40 wt% in the case of Si) catalyst (if used), EG : PET ratio of 16, 2 h. BHET yield was determined by HPLC.

ments, so a  $2^{4-1}$  experimental design was developed to describe the variation of the dependent variable, non-isolated BHET yield, as a function of the independent parameters using a linear regression model. Si-TEA catalyst was used during the experiments because of its highest thermal stability among the investigated modified silica gels and appropriate activity. The lower and upper levels of the parameters were chosen based on preliminary experiments by changing the parameters one by one (see Fig. S13–S15 in the ESI†) to obtain an approximately linear relationship between the dependent variable and the parameters in the chosen parameter ranges. Their coded and uncoded values are shown in Table 2. The experimental design matrix and the observed BHET yields and PET conversions from 20 experiments are presented in Table 3.

In the fractional design, the triple interaction between temperature, catalyst : PET ratio and EG : PET ratio is confounded with the fourth factor (reaction time). In this case, the main effects are not mixed with each other or with two-factor interactions, while the two-factor interactions are confounding with each other ( $A$  by  $B$  with  $C$  by  $D$ ;  $A$  by  $C$  with  $B$  by  $D$ ;  $A$  by  $D$  with  $B$  by  $C$ ). Since out of the interactions, only  $A$  by  $D$  (and its linear combination,  $B$  by  $C$ ) were found to be significant, the  $B$  by  $C$  interaction was chosen as the only significant interaction based on practical considerations ( $B$  by  $C$  interaction is the interaction of catalyst quantity and EG : PET ratio, which influences the catalyst concentration in the reaction mixture). The results of ANOVA for the regression model are shown in Table 4. A factor is considered significant if its  $p$ -value is less than 0.05, and the higher the  $F$ -value, the greater the signifi-

cance of its effect on the model response. Thus, all the main effects and the  $B$  by  $C$  interaction effect were found to be significant. The Pareto charts of standardised effects in the case of BHET yield or PET conversion as the dependent variable can be found in Fig. S16 and S17 in the ESI.†

After model reduction by removing the statistically insignificant factors, a new linear regression model was fitted to the experimental data, and it proved to be adequate based on the curvature check with a high value of  $R^2$  (0.969) and adjusted  $R^2$  (0.955). Analysis of variance for the reduced linear regression model can be seen in Table S3 in the ESI.† Comparing the yields estimated from the model and the observed ones, it was found that the measured points are approximately along a line of slope 1 through the origin (Fig. 4), therefore the regression model was adequate for predicting the BHET yield in the design space, especially at high yields. The homogeneity of variances was checked comparing the predicted and residual values of BHET yield (see Fig. S18 in the ESI†), and using a Cochran's  $C$  test (see ESI†). Based on the latter, the assumption that the random error variance is constant can be accepted. Taking this into account, the reduced model can be used to determine the optimal conditions.

The reduced linear regression model representing the relationship between the BHET yield response  $Y$  and the coded values of the four independent factors was obtained as

$$Y = 39.8 + 30.6A + 12.7B - 11.9C + 13.4D + 4.2BC \quad (4)$$

Based on this model, the temperature ( $A$ ) has the strongest effect on the BHET yield, while the interaction of catalyst ratio and EG ratio ( $BC$ ) has low significance.

The interaction between catalyst : PET ratio and EG : PET ratio at a constant temperature of 190 °C and with a reaction time of 2 h was plotted in Fig. 5 on a response surface plot (a function of two factors with the others at constant values). At a fixed catalyst ratio, the yield decreases with increasing EG ratio in this investigating range. It should be noted, however, that in our preliminary experiments, we found that the yield has a maximum at a certain EG ratio value. For this, the explanation could be that the transformation of dimer into monomer is a reversible process. Therefore, prolonging the reaction after reaching equilibrium can cause a backward shift, increasing the amount of dimer at the expense of the BHET monomer.<sup>50</sup> In this case, the higher ratio of EG presumably shifted the equilibrium faster towards the dimer. In the design of experiments, however, the factor values were chosen so that there was an approximately linear relationship between yield and EG ratio. On the surface plot, the interaction can be observed that at a lower catalyst ratio, the EG ratio has a greater negative effect on yield than at a higher catalyst ratio, and similarly, at a higher EG ratio, the catalyst ratio has a greater positive effect on yield than at a lower EG ratio.

**Table 2** Coded and uncoded levels of independent variables

Independent variables	Factor	Coded level		
		−1	0	+1
Temperature (°C)	$A$	170	180	190
Catalyst : PET ratio (mol%)	$B$	5	12.5	20
EG : PET molar ratio (−)	$C$	11	13.5	16
Reaction time (h)	$D$	1	1.5	2

### 3.4 Optimisation of reaction conditions

The optimisation was implemented using response surface methodology with gradient method. Accordingly, with the step



**Table 3** Experimental design matrix and observed BHET yield and PET conversion

Run	Temperature (°C)	Catalyst : PET ratio (mol%)	EG : PET molar ratio (-)	Reaction time (h)	Conversion (%)	BHET yield (%)
1	170	5.0	11.0	1.0	1	0
2	190	5.0	11.0	2.0	100	88
3	170	20.0	11.0	2.0	51	45
4	190	20.0	11.0	1.0	94	80
5	170	5.0	16.0	2.0	1	0
6	190	5.0	16.0	1.0	34	28
7	170	20.0	16.0	1.0	1	0
8	190	20.0	16.0	2.0	100	90
9 (C)	180	12.5	13.5	1.5	38	31
10 (C)	180	12.5	13.5	1.5	58	51
11	170	5.0	11.0	1.0	5	0
12	190	5.0	11.0	2.0	97	85
13	170	20.0	11.0	2.0	37	29
14	190	20.0	11.0	1.0	100	87
15	170	5.0	16.0	2.0	7	0
16	190	5.0	16.0	1.0	21	16
17	170	20.0	16.0	1.0	8	0
18	190	20.0	16.0	2.0	99	89
19 (C)	180	12.5	13.5	1.5	46	41
20 (C)	180	12.5	13.5	1.5	45	40

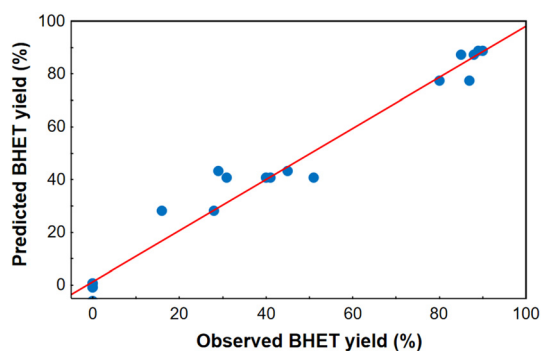
C: centre point.

**Table 4** Analysis of variance for linear regression model

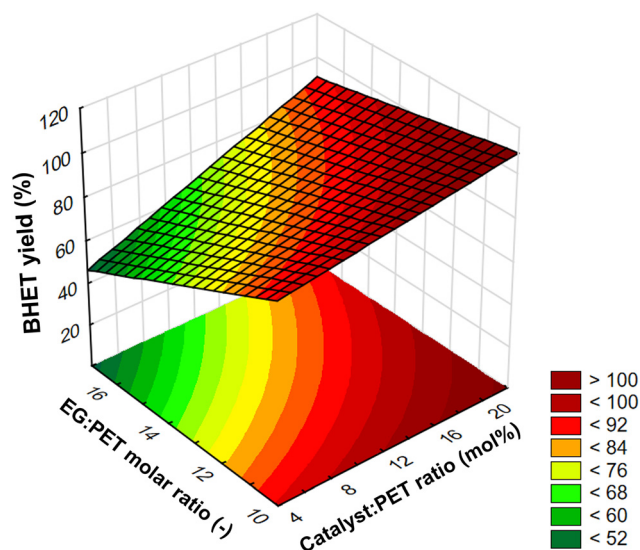
Factor	Sum of squares	DF	Mean square	F-Value	p-Value	Significant
Curvature	2.81	1	2.81	0.07	0.7935	No
(A) Temperature (°C)	14 945.06	1	14 945.06	382.09	<0.0001	Yes
(B) Catalyst : PET ratio (mol%)	2575.56	1	2575.56	65.85	<0.0001	Yes
(C) EG : PET ratio (-)	2280.06	1	2280.06	58.29	<0.0001	Yes
(D) Reaction time (h)	2889.06	1	2889.06	73.86	<0.0001	Yes
A by B	189.06	1	189.06	4.83	0.0502	No
A by C	115.56	1	115.56	2.95	0.1136	No
B by C	280.56	1	280.56	7.17	0.0215	Yes
Error	430.25	11	39.11			

Total sum of squares 23 708.0019

DF: degree of freedom.

**Fig. 4** Comparison of observed and predicted BHET yields.

intervals chosen adequately, steps are taken from the centre point of the design space towards the local maximum along the gradient of the reduced model because this is the direction of steepest ascent. The temperature step interval was chosen as the determining one (since this is the most difficult to set to a certain value), which is 2.5 °C in all cases. The step inter-

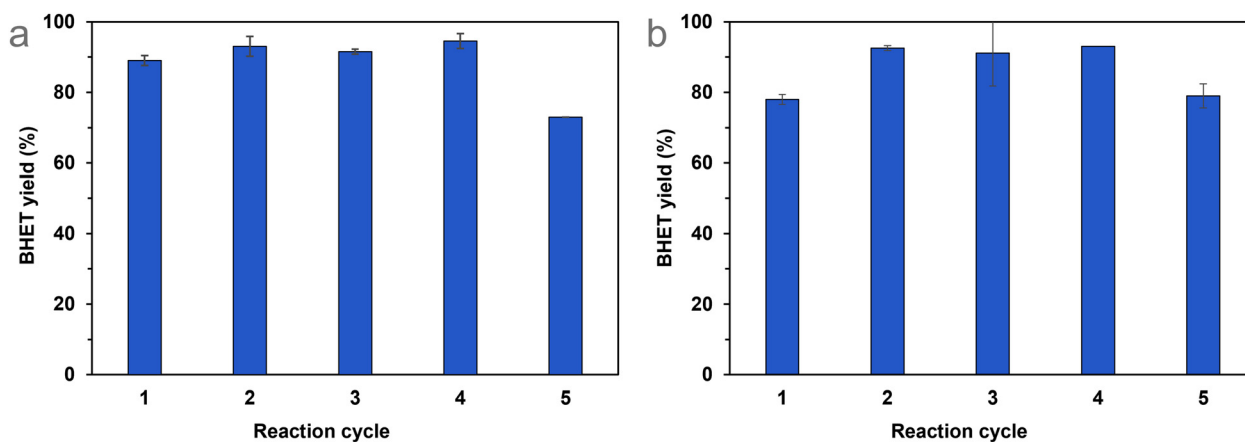
**Fig. 5** Response surface plot for the interaction effect between catalyst : PET ratio and EG : PET ratio at a constant temperature of 190 °C and with a reaction time of 2 h.





**Table 6** Comparison of PET glycolysis methods using experimental design. The optimal reaction conditions are indicated, and the parameter ranges investigated are given in parentheses

Ref.	Catalyst	Design	Temperature (°C)	Reaction time (h)	Catalyst : PET molar ratio (%)	EG : PET molar ratio (–)	Conversion (%)	Yield (%)
Ref. 36	Co(OAc) <sub>2</sub>	2 <sup>3</sup>	190 (130–190)	2.0 (0.5–2)	1.0 (0–1)	6.2 ( <i>fixed</i> )	100	n.d.
Ref. 37	Mn(OAc) <sub>2</sub>	2 <sup>3</sup>	190 (130–190)	1.5 (0.5–2)	0.5 (0.05–0.5)	6.2 ( <i>fixed</i> )	100	n.d.
Ref. 38	Zn(OAc) <sub>2</sub>	Taguchi L <sub>9</sub>	208 (195–220)	2.5 (2.5–3.5)	0.2 (0.2–1)	18.6 (6.2–18.6)	n.d.	85
Ref. 41	Zn(OAc) <sub>2</sub>	Taguchi L <sub>20</sub>	250 ( <i>MW</i> ) ( <i>fixed</i> )	0.5 ( <i>fixed</i> )	1.0 (1–4)	9.3 (3.1–15.5)	n.d.	65
Ref. 40	NaHCO <sub>3</sub>	4 factor Box–Behnken design	192 (192–200)	3.0 (3–5)	1.9 (1.4–2.3)	18.8 (7.7–23.2)	n.d.	75.7
This work	Si-TEA	2 <sup>4-1</sup>	190 (170–195)	1.7 (1–2)	15.5 (5–20)	12.6 (11–16)	100	88.5

**Fig. 7** Catalyst recycling in PET glycolysis applying Si-TEA (a) and Si-TBD (b) catalysts.

cant catalytic activity loss during the catalyst recycling experiments.

Stabilities of Si-TEA and Si-TBD catalysts were further investigated by HS-GC-MS, and only a small amount of amines were detected as decomposition products only in the case of Si-TEA. After a 4-hour glycolysis reaction under optimised conditions, we detected a very low amount of different amines (triethylamine, diethylmethylamine, diethylamine) compared to a triethylamine reference, which contained 5% of the TEA amount grafted onto the silica gel (Fig. S19 and 20†). Their peak areas can be seen in Table S6† (those fragments of the detected compounds were depicted on the chromatogram, which had approximately the same intensities considering the mass spectra of the amines; thus, it gives a relative quantitative estimation for the decomposition products). Besides amines, acetone and methyl 1,3-dioxolane (product of the reaction of ethylene glycol and acetaldehyde – the latter is a by-product of PET degradation reactions<sup>53</sup>) were detected. In the case of Si-TBD, no decomposition products were detected by HS-GC-MS. All reaction mixtures were also analysed by HPLC-MS, and no decomposition products were detected in the case of Si-TEA. However, in the case of Si-TBD, trace amounts of TBD were detected, but only by the first application of the catalyst. After catalyst recycling, it could not be detected.

Thus, we assume that the reason for the slight catalyst mass loss (see Table S5†) is that smaller-sized particles separ-

ate from the irregular shaped silica gel at high temperature while stirring in the polar ethylene glycol. These particles go through the G3 porosity glass filter, thus causing the catalyst mass loss. To examine this, we recovered some of the lost catalyst when a large amount of water was added to the filtrate (see Section 2.3), and the precipitate was found to contain Si-TEA. A catalyst recycling experiment was conducted with this recovered smaller-sized Si-TEA, which remained active (64% non-isolated BHET yield in the case of 5 mol% Si-TEA). It should be noted, however, that the lost catalyst was difficult to recover and still contained BHET dimer after washing with a methanol/ethyl acetate mixture. Consequently, future studies should focus on examining the stability of spherical silica gels and other types of catalyst carriers.

Based on the work of Thielemans and co-workers,<sup>9</sup> the environmental energy impact ( $\xi$ , eqn (5)) value equals the quotient of the environmental factor ( $E_{\text{factor}}$ ) and the energy economy factor ( $\epsilon$ ). This green chemistry metric has allowed for quantitative comparison between different studies and for determining their relative feasibility. The lower the environmental energy impact, the more favourable the technology is, since the  $E_{\text{factor}}$  is equal to the mass of waste divided by the mass of product, and the energy economy factor is equal to the yield divided by the temperature times the reaction time (see Section 8 in the ESI†). Comparing Si-TEA and Si-TBD to other organocatalysts (Table 7, and Table S7† in more detail),



**Table 7** Comparing the environmental energy impact,  $E_{\text{factor}}$  and energy economy factor of Si-TEA and Si-TBD to organocatalysts applied in PET glycolysis

Ref.	Catalyst	$\xi$ ( $^{\circ}\text{C min}$ )	$E_{\text{factor}}$ (-)	$\epsilon$ ( $^{\circ}\text{C}^{-1} \text{min}^{-1}$ )
Ref. 25	TBD	24938 <sup>9</sup>	0.4875	$1.955 \times 10^{-5}$
Ref. 23	TBD : MSA	12911 <sup>9</sup>	0.5440	$4.213 \times 10^{-5}$
This work	Si-TEA	7585	0.3483	$4.592 \times 10^{-5}$
	Si-TBD	7758	0.3523	$4.541 \times 10^{-5}$

MSA: methanesulfonic acid.

their environmental energy impacts, environmental factors, and energy economy factors are slightly better, so these catalysts can be feasible alternative catalysts in PET glycolysis. The cumulative BHET yields (for five reaction cycles) were applied in the calculations, and the catalysts were not included in the waste mass because of their recyclability (at a certain reaction cycle number, the catalyst mass can be neglected) (see ESI<sup>†</sup>), as also reported in the work of Thielemans.

$$\xi = \frac{E_{\text{factor}}}{\epsilon} (^{\circ}\text{C min}) \quad (5)$$

While most heterogeneous catalysts applied in PET glycolysis do not often maintain high BHET selectivity and require higher temperatures than most other catalysts,<sup>51</sup> in this work, high selectivity was maintained in 5 reaction cycles at only 190  $^{\circ}\text{C}$ . In the future, catalyst recycling in more cycles will be performed on a larger scale.

### 3.6 Preliminary scale-up of PET glycolysis process

To examine the achievable yield and how much longer it takes to depolymerise PET on a larger scale under the previously optimised conditions at small scale, a 6-fold scale-up was applied using Si-TEA catalyst at 190  $^{\circ}\text{C}$ , and the catalyst : PET ratio and the EG : PET ratio were adjusted to the optimal values as previously determined (see detailed description of the scale-up in Section 2.5). The reaction time was increased to 2.5 h, as the reaction mixture still visibly contained PET particles after 1.7 h, which was the optimal time for the smaller size. Full conversion was achieved, and the preparative BHET yield was 74% (meaning that the BHET dimer was still present in the reaction mixture after the reaction time of 2.5 h). The slightly lower preparative BHET yield could probably be attributed to the non-optimal reaction time because of the sub-optimal stirring on the larger scale, suggesting that further optimisation of the scale-up reaction time or stirring speed is required in order to obtain higher monomer selectivity and yield. Although this reaction size is still far from the industrial scale, the results suggest that the method may be suitable for the degradation of PET waste on larger scale.

Using the unmodified silica gel (Si) as a catalyst, 34% PET conversion and 26% non-isolated BHET yield were achieved in 2 h reaction time during the catalyst screening experiments (see Fig. 3). Since silica gel is cheaper and thermally more stable than functionalized silica gels, its application in the gly-

colysis of PET was further investigated. Silica gel was used as a catalyst in a 6-fold scale-up reaction at 50 wt%. The reaction was carried out at 190  $^{\circ}\text{C}$ , using an EG : PET ratio of 12.6 in 10 h reaction time since the PET particles were broken down in the reaction mixture during this time. Under these conditions, complete conversion and 72% BHET yield were obtained, *i.e.*, the silica gel could be successfully used as a catalyst for the process. Nevertheless, the reaction took significantly more time, showing that silica gels functionalized with organic moieties have a much higher catalytic activity, and thus their application on an industrial scale may be more advantageous in terms of energy savings.

To prove the feasibility of scaling-up by using mechanical stirring, an 18-fold scale-up experiment was performed with mechanical stirring for 5 hours. The glycolysis reaction gave full conversion, 83% HPLC yield of BHET, and 72% isolated BHET yield by crystallization. The isolated BHET yield could be further increased by 7% (79% in sum) by column chromatography. Then, further side-products besides dimer of BHET were identified by HPLC-MS: BHET trimer, 2-hydroxyethyl terephthalic acid (in a higher proportion than the rest), and 2-(2-hydroxyethoxy)ethyl (2-hydroxyethyl) terephthalate (Fig. S12 and Table S2<sup>†</sup>). As only one experiment was performed, which was stopped based on the disappearance of PET flakes, the reaction time of the scaled-up reaction needs to be further optimised in the future.

These findings serve as preliminary studies for future scale-up optimisation. Glycolytic PET depolymerisation is already applied on pilot and even commercial scales,<sup>5</sup> however, these processes have limitations: using catalysts is not preferred because of the issues associated with their often difficult recovery and high cost, and in the case of mixed PET waste processes, the removal of pigments and dyes is problematic.<sup>54</sup> In our work, catalyst recovery is a crucial aspect, and by using solid-supported organocatalysts, their reuse is made more straightforward as they can be recycled by simple filtration. An issue is the catalyst loss, which will be addressed in the future, and investigating the depolymerisation of mixed PET waste streams is also planned. Later, the nature of the support can also be optimised to address, *e.g.*, issues of the catalyst recovery or the cost of the catalyst. The recovery of ethylene glycol was reported in earlier studies,<sup>23,44</sup> this will be also investigated in the future scale-up optimisation.

## 4. Conclusions

In this work, three commercially available functionalized silica gels and a newly synthesised one, namely solid-supported TBD, were tested as heterogeneous organocatalysts in PET glycolysis. Si-TEA was found to have the highest thermal stability based on TG-DSC and good catalytic activity, while Si-TBD had the highest activity. The effects of four parameters were investigated by experimental design, and a simple linear model was set up to represent the relationship between the BHET yield and the coded values of the four independent factors. The





- 20 F. Scé, I. Cano, C. Martin, G. Beobide, O. Castillo and I. De Pedro, *New J. Chem.*, 2019, **43**, 3476–3485.
- 21 F. R. Veregue, C. T. P. da Silva, M. P. Moisés, J. G. Meneguín, M. R. Guilherme, P. A. Arroyo, S. L. Favaro, E. Radovanovic, E. M. Giroto and A. W. Rinaldi, *ACS Sustainable Chem. Eng.*, 2018, **6**, 12017–12024.
- 22 P. Fang, B. Liu, J. Xu, Q. Zhou, S. Zhang, J. Ma and X. lu, *Polym. Degrad. Stab.*, 2018, **156**, 22–31.
- 23 C. Jehanno, I. Flores, A. P. Dove, A. J. Müller, F. Ruipérez and H. Sardon, *Green Chem.*, 2018, **20**, 1205–1212.
- 24 M. Blümel, J. M. Noy, D. Enders, M. H. Stenzel and T. V. Nguyen, *Org. Lett.*, 2016, **18**, 2208–2211.
- 25 K. Fukushima, D. J. Coady, G. O. Jones, H. A. Almegren, A. M. Alabdulrahman, F. D. Alsewaleim, H. W. Horn, J. E. Rice and J. L. Hedrick, *J. Polym. Sci., Part A: Polym. Chem.*, 2013, **51**, 1606–1611.
- 26 I. Cano, C. Martin, J. A. Fernandes, R. W. Lodge, J. Dupont, F. A. Casado-Carmona, R. Lucena, S. Cardenas, V. Sans and I. de Pedro, *Appl. Catal., B*, 2020, **260**, 118110.
- 27 Y. Liu, X. Yao, H. Yao, Q. Zhou, J. Xin, X. Lu and S. Zhang, *Green Chem.*, 2020, **22**, 3122–3131.
- 28 J. Sun, D. Liu, R. P. Young, A. G. Cruz, N. G. Isern, T. Schuerg, J. R. Cort, B. A. Simmons and S. Singh, *ChemSusChem*, 2018, **11**, 781–792.
- 29 A. M. Al-Sabagh, F. Z. Yehia, G. Eshaq and A. E. ElMetwally, *Ind. Eng. Chem. Res.*, 2015, **54**, 12474–12481.
- 30 R. Wang, T. Wang, G. Yu and X. Chen, *Polym. Degrad. Stab.*, 2021, **183**, 109463.
- 31 E. Sert, E. Yilmaz and F. S. Atalay, *J. Polym. Environ.*, 2019, **27**, 2956–2962.
- 32 B. Liu, W. Fu, X. Lu, Q. Zhou and S. Zhang, *ACS Sustainable Chem. Eng.*, 2019, **7**, 3292–3300.
- 33 Q. Wang, X. Yao, Y. Geng, Q. Zhou, X. Lu and S. Zhang, *Green Chem.*, 2015, **17**, 2473–2479.
- 34 L. D. Ellis, N. A. Rorrer, K. P. Sullivan, M. Otto, J. E. McGeehan, Y. Román-Leshkov, N. Wierckx and G. T. Beckham, *Nat. Catal.*, 2021, **4**, 539–556.
- 35 H. Sardon, M. Valle, X. Lopez de Pariza, M. Ximenis and J. M. W. Chan, *Angew. Chem., Int. Ed.*, 2022, e202203043.
- 36 C.-H. Chen, C.-Y. Chen, Y.-W. Lo, C.-F. Mao and W.-T. Liao, *J. Appl. Polym. Sci.*, 2001, **80**, 956–962.
- 37 C.-H. Chen, *J. Appl. Polym. Sci.*, 2003, **87**, 2004–2010.
- 38 A. Aguado, L. Martínez, L. Becerra, M. Arieta-araunabeña, S. Arnaiz, A. Asueta and I. Robertson, *J. Mater. Cycles Waste Manage.*, 2014, **16**, 201–210.
- 39 D. M. Scremin, D. Y. Miyazaki, C. E. Lunelli, S. A. Silva and S. F. Zawadzki, *Macromol. Symp.*, 2019, **383**, 1800027.
- 40 D. T. Van-Pham, Q. H. Le, T. N. Lam, C. N. Nguyen and W. Sakai, *Polym. Degrad. Stab.*, 2020, **179**, 109257.
- 41 R. Park, V. Sridhar and H. Park, *J. Mater. Cycles Waste Manage.*, 2020, **22**, 664–672.
- 42 A. Stoski, M. F. Viante, C. S. Nunes, E. C. Muniz, M. L. Felsner and C. A. P. Almeida, *Polym. Int.*, 2016, **65**, 1024–1030.
- 43 S. Katoch, V. Sharma, P. P. Kundu and M. B. Bera, *ISRN Polym. Sci.*, 2012, **2012**, 1–9.
- 44 Q. Wang, X. Yao, S. Tang, X. Lu, X. Zhang and S. Zhang, *Green Chem.*, 2012, **14**, 2559–2566.
- 45 M. Ferré, R. Pleixats, M. Wong Chi Man and X. Cattoën, *Green Chem.*, 2016, **18**, 881–922.
- 46 A. Chuma, H. W. Horn, W. C. Swope, R. C. Pratt, L. Zhang, B. G. G. Lohmeijer, C. G. Wade, R. M. Waymouth, J. L. Hedrick and J. E. Rice, *J. Am. Chem. Soc.*, 2008, **130**, 6749–6754.
- 47 K. Fukushima, O. Coulembier, J. M. Lecuyer, H. A. Almegren, A. M. Alabdulrahman, F. D. Alsewaleim, M. A. McNeil, P. Dubois, R. M. Waymouth, H. W. Horn, J. E. Rice and J. L. Hedrick, *J. Polym. Sci., Part A: Polym. Chem.*, 2011, **49**, 1273–1281.
- 48 R. Srivastava, *J. Mol. Catal. A: Chem.*, 2007, **264**, 146–152.
- 49 R. D. Allen, K. M. Bajjuri, G. Breyta, J. L. Hedrick and C. E. Larson, WO2015/056377A1, 2015.
- 50 A. Sheel and D. Pant, in *Recycling of Polyethylene Terephthalate Bottles*, ed. S. Thomas, A. V. Rane, K. Kanny, V. K. Abitha and M. G. Thomas, William Andrew Publishing, 2019, pp. 61–84.
- 51 S. C. Kosloski-Oh, Z. A. Wood, Y. Manjarrez, J. P. de los Rios and M. E. Fieser, *Mater. Horiz.*, 2021, **8**, 1084–1129.
- 52 P. T. Nguyen, B. Nohair, N. Mighri and S. Kaliaguine, *Microporous Mesoporous Mater.*, 2013, **180**, 293–300.
- 53 A. M. Al-Sabagh, F. Z. Yehia, G. Eshaq, A. M. Rabie and A. E. ElMetwally, *Egypt. J. Pet.*, 2016, **25**, 53–64.
- 54 T. Thiounn and R. C. Smith, *J. Polym. Sci.*, 2020, **58**, 1347–1364.

